

Tunable Hydrogels for External Manipulation of Cellular Microenvironments through Controlled Photodegradation

By April M. Kloxin, Mark W. Tibbitt, Andrea M. Kasko, Jonathan A. Fairbairn, and Kristi S. Anseth*

Hydrogels provide a unique environment for three-dimensional cell culture, but typically, the material properties are fixed upon formation. Given the growing interest in understanding how material microenvironments influence cellular functions, numerous approaches have emerged to control not only the initial biochemical and biophysical properties of gels, but also how these properties change with degradation. While these strategies allow the synthesis of hydrogels with predictable degradation profiles and property changes, a material system that allows external manipulation of the properties of a cell-laden gel at any point in time or space would fill a unique niche. For example, such a cell culture system would allow real-time manipulation of the extracellular microenvironment and simultaneous monitoring of cellular processes in three-dimensional culture. In this contribution, photocleavable linkers were integrated into the crosslinks of a poly(ethylene glycol)-based (PEG) hydrogel, allowing the network structure to be tuned exogeneously and predictably with irradiation under cytocompatible conditions. Such a material system will enable new opportunities to test hypotheses about how precise variations in the local gel environment direct important cellular functions, such as process extension, migration, and mechanotransduction.

There is a growing interest in the development of hydrogels as a platform for encapsulating cells and their application in fields ranging from tissue engineering to three-dimensional cell culture.^[1] As one example, di(meth)acrylated PEG macromolecules can be polymerized via photoinitiation to form a hydrogel in the presence of cells,^[2] and these covalently crosslinked materials have been widely used in numerous tissue engineering applications.^[3–5] Beyond simple cell encapsulation, Hahn et al.^[6] reported the chemical patterning of these PEG networks using a two-photon confocal laser scanning microscope (LSM).

Using a two-step process, an RGD functionalized PEG network was formed in spatially defined regions within an existing PEG gel. More recently, Tayalia et al.^[7] demonstrated the potential of two-photon initiation to spatially direct polymerization of multifunctional acrylate monomers. Networks with uniform pores ranging from 10 to 100 μm were fabricated, allowing the examination of cell migration as a function of pore size. While control of the initial network structure and chemistry is important for cell culture scaffolds, an equally fundamental aspect of hydrogel design is temporal regulation of the material properties (i.e., degradation).

Hydrogel property control via degradation is critical, as many dynamic cellular processes require temporal and spatial changes in the material environment. Changes in hydrogel properties, such as crosslinking density and modulus, allow and even dictate changes in cell functions such as migration,^[8] process extension,^[9] and differentiation.^[10] Degradation of PEG hydrogels is often achieved by incorporating hydrolytically or enzymatically degradable blocks within the gel-forming macromers. Classically, hydrolytically degradable gels have been synthesized from poly(lactic acid)-*b*-PEG-*b*-poly(lactic acid) (PLA-*b*-PEG-*b*-PLA) and poly(caprolactone)-*b*-PEG-*b*-poly(caprolactone) (PCL-*b*-PEG-*b*-PCL) macromers with vinyl end groups, where the temporal degradation rate is dictated by the initial macromer chemistry.^[11–13] While this chemistry leads to hydrogels with predictable changes in their material properties with time, the process occurs uniformly in the bulk and cannot be altered after gel formation. More recently, enzymatically degradable gels have been created from PEG macromers containing matrix metalloprotease-degradable (MMP) peptide blocks or through a step-growth reaction of thiol-functionalized oligopeptides with vinyl functionalized PEGs.^[10,14] In these materials, cells secrete MMPs and locally dictate the degradation rate. This mechanism provides specific advantages for many tissue engineering applications, as the gel degradation does not need to be fixed *a priori*. However, the experimenter cannot easily manipulate the cellular microenvironment, and understanding how the cells are manipulating their local material environment is challenging. Thus, a three-dimensional cell culture system that would allow externally regulated changes in the gel structure and properties in time and space would address a void in current biomaterial scaffolds.

Light-induced reactions have the potential to offer this level of temporal and spatial material property control. Literature demonstrates that hydrogels formed by dimerization of nitro-cinnamate groups afford reversible hydrogel formation but require cytotoxic irradiation conditions (254 nm light).^[15,16] To

[*] Prof. K. S. Anseth, Prof. A. M. Kasko^[†]
Department of Chemical and Biological Engineering and the Howard Hughes Medical Institute
University of Colorado at Boulder
424 UCB, ECCH 111, Boulder, CO 80309 (USA)
E-mail: kristi.anseth@colorado.edu

Dr. A. M. Kloxin, M. W. Tibbitt, J. A. Fairbairn
Department of Chemical and Biological Engineering
University of Colorado at Boulder 424 UCB, ECCH 111, Boulder, CO 80309 (USA)

[†] Present address: Department of Bioengineering, University of California, Los Angeles, CA 90095-1600, USA

DOI: 10.1002/adma.200900917

avoid use of this cytotoxic wavelength, researchers have incorporated nitrobenzyl ether derivatives within hydrogels, which cleave upon exposure to 365 nm light for post-gelation modification with pendant functionalities.^[17] Recently, we have incorporated this photolabile moiety into PEG-based hydrogels to control gel erosion and the presentation of an adhesion peptide.^[18] Here, we demonstrate that this chemistry affords precise and predictable tuning of the gel structure in real-time with low-intensity, long-wavelength UV light under cytocompatible conditions. Specifically, gradients in crosslinking density are created and utilized to control cell morphology in three-dimensions, and mass loss and gel erosion are controlled and predicted using a photodegradation model. Further, by focusing a single-photon visible light source, the desired properties are manipulated in three-dimensions with micrometer-scale resolution.

Photodegradable PEG-based hydrogels containing a nitrobenzyl ether photolabile moiety^[19,20] were synthesized by redox-initiated radical chain copolymerization of a diacrylated PEG-based photodegradable crosslinking macromer (PEGdiPDA)^[18] with a monoacrylated PEG (PEGA) in water. The molar ratio of PEGdiPDA to PEGA was varied to alter the initial gel crosslinking density (Fig. 1). Upon irradiation, the photocleavable crosslinks degrade, releasing modified PEG and decreasing the crosslinking density until complete dissolution at the reverse gel point.^[21] Depending on the irradiation wavelength and concentration of the photodegradable group in the swollen gel, light can either penetrate uniformly, leading to bulk degradation (Fig. 1b, top), or become attenuated, leading to gradient changes in the crosslinking density (Fig. 1b, middle) or surface erosion (Fig. 1b, bottom). At commonly used wavelengths for cell encapsulation and imaging, the molar extinction coefficients of the photodegradable group decrease from 7600 L mol⁻¹ cm⁻¹ at 365 nm to 1640 L mol⁻¹ cm⁻¹ at 405 nm to 73 L mol⁻¹ cm⁻¹ at 488 nm. Based on the photolabile moiety's light absorbance and quantum yield, the irradiation wavelength and intensity dictate the degradation rate and are used to predictably tune the hydrogel properties in time and space. In addition, light can be focused within the hydrogel using a single photon LSM, eroding the gel only near the focal point and allowing subsequent rastering of the focal point within the gel to create three-dimensional structures (Fig. 1c).

To characterize the hydrogel's degradation kinetics, the bulk degradation of optically thin gels was followed with rheometry during irradiation. The hydrogel elasticity (the storage modulus, G') scales with the gel crosslinking density (ρ_x), and, from this,

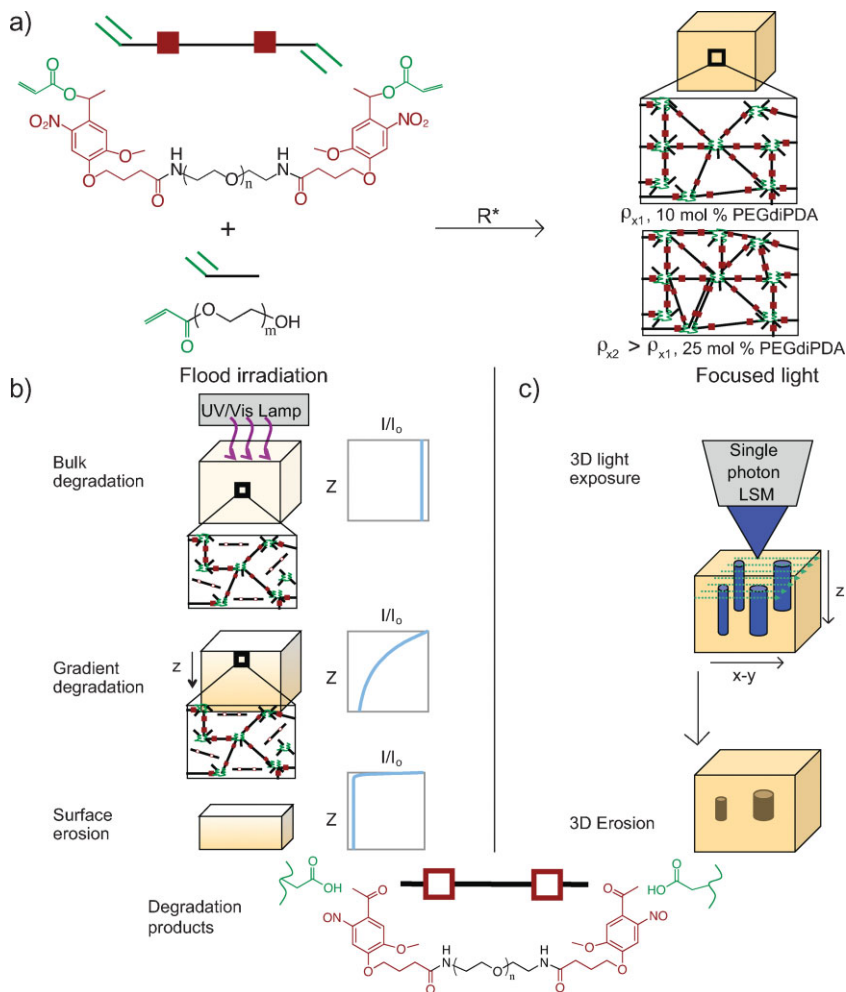


Figure 1. Photodegradable hydrogel synthesis and degradation schematics. a) Photodegradable hydrogels were synthesized by redox-initiated radical chain polymerization of PEGdiPDA (top left) with PEGA (bottom left) (15 wt% total macromer in water). The resulting swollen polymer network consists of polyacrylate chains (green coils) linked by degradable PEG (black lines with red boxes). The initial gel crosslinking density (ρ_x) is varied with crosslinker concentration. b) Upon irradiation, the photolabile moiety is cleaved (open red boxes), releasing PEG (black) and decreasing the gel crosslinking density. With flood irradiation, light can either penetrate the gel uniformly, causing bulk degradation (top), or be attenuated with absorption by the photolabile group, causing gradient changes in the crosslinking density (middle) or surface erosion (bottom). The intensity profile within the gel is dictated by the irradiation wavelength and the photolabile group concentration. c) Three-dimensional structures are eroded in a hydrogel using focused light directed by a single photon LSM, where desired shapes are drawn using region of interest software and subsequently scanned with a laser within the hydrogel.

the photolabile group characteristic degradation time constant (τ) was calculated (Eq. 1).

$$\ln\left(\frac{G'}{G'_0}\right) = \ln\left(\frac{\rho_x}{\rho_{x_0}}\right) = -\frac{2t}{\tau} \quad (1)$$

Here, G'_0 is the initial storage modulus, ρ_{x_0} the initial crosslinking density, and t the irradiation time. The factor of 2 is included as cleavage of the photodegradable group on either side of the PEG leads to a decrease in the network's crosslinking

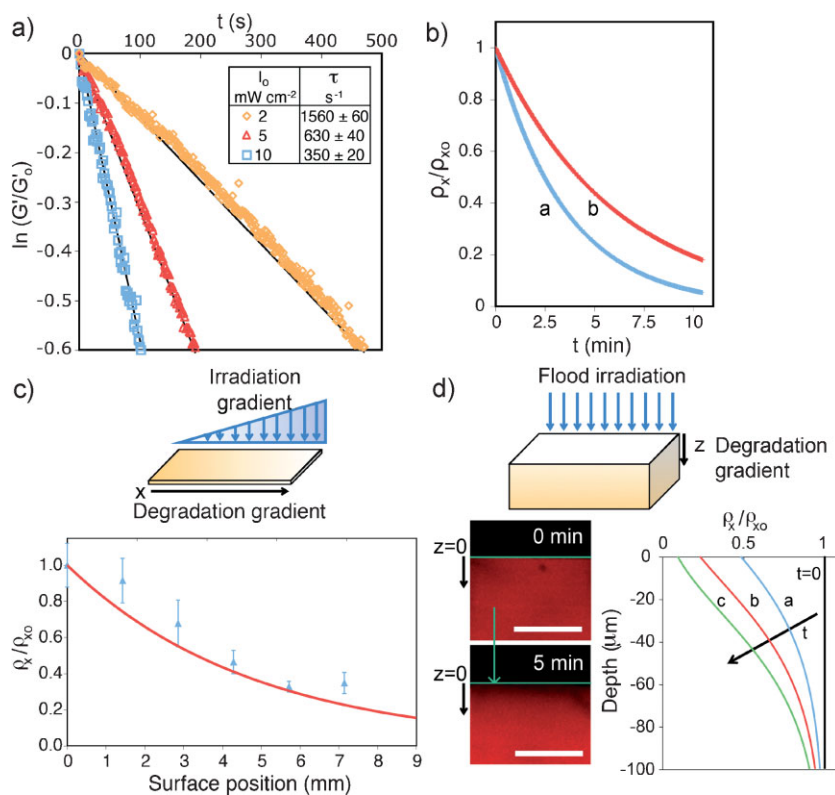


Figure 2. Photolysis kinetics and gradient photodegradation. a) Degradation of these hydrogels was characterized using the more loosely crosslinked gel composition (10 mol %: 90 mol % PEGdiPDA: PEGA). Photodegradation rates were characterized with rheometry, where the natural log of the storage modulus G' normalized to its initial value G'_0 decreases with 365 nm irradiation. Fits of this data yield the characteristic degradation time, τ , which varies with the irradiation intensity (inset) and was used in conjunction with a photodegradation model to predict changes in the hydrogel crosslinking as well as gel mass loss. b) The experimentally determined τ values were used to predict the hydrogel's crosslinking density with time during bulk degradation (normalized to initial value, (a) 10 mW cm⁻² and (b) 5 mW cm⁻² at 365 nm). c) A gradient in the hydrogel's crosslinking density within the top 50 μm of the gel was created with an irradiation gradient across the surface. No degradation occurs on the left, 5 min of degradation occurs on the right, and a continuous and linear gradient of exposure times occurs between these two extremes (365 nm at 10 mW cm⁻²). The resulting crosslinking density gradient was measured with AFM (blue triangles) and compares well to predicted values based on τ (solid curve). d) Flood irradiating a thick hydrogel with a highly absorbed wavelength creates a degradation gradient in the z -direction within the hydrogel. This degradation gradient was visualized with a confocal LSM (left), where decreased fluorescence indicates loss of backbone chains. The effect of this degradation gradient on the material properties can be estimated through predicted changes in the crosslinking density (normalized to its initial value) with irradiation: (a) 2.5, (b) 5, and (c) 8 min (right). Scale bars are 100 μm .

density. τ scales inversely with the incident light intensity, I_0 , and the photolabile molecule's molar absorptivity (ϵ).^[22,23] The characteristic degradation times for several cytocompatible light conditions^[24] were determined with rheometry (Fig. 2a). Using these τ values, hydrogel photodegradation and changes in commensurate material properties, such as crosslinking density, over time (Fig. 2b) were predicted.

Spatial property gradients were achieved in the x - y plane or z -direction by controlling the light exposure and intensity, respectively. A surface gradient was created by moving an opaque plate across the sample during irradiation to create a linear gradient in exposure time from 0 (at 0 mm) to 5 min (at 9 mm).

both the degradation kinetics (τ) and overall network connectivity. In particular, the time to reach the reverse gel point (complete dissolution), t_{rev} depends on several factors: (i) the wavelength and intensity of irradiation and hydrogel thickness, which adjust τ and the intensity profile within the hydrogel due to light attenuation; (ii) the length of the polyacrylate backbone chains comprising the network; and (iii) the connectivity of the polyacrylate chains dictated by the initial amount of crosslinker.

To examine these effects on the time to reach reverse gelation, thick hydrogels that undergo mass loss via surface erosion when exposed to a highly absorbing wavelength were synthesized. The mass loss profiles were adjusted with the initial crosslinker

The resulting degradation-induced crosslinking density gradient was measured with AFM and compares well to predictions based on τ (Fig. 2c). A gradient within the gel was fabricated using an optically thick sample, where the photolabile group substantially attenuates the light intensity over the hydrogel thickness. In this example, <1% of the incident light at the surface is transmitted at a depth of 100 μm . To characterize this gradient with depth, the backbone of the polymer network was covalently labeled with rhodamine. As the gel degrades, PEG is released, along with PEG attached to the fluorescently labeled polyacrylate backbone chains. As imaged with a confocal LSM, uniform fluorescence is initially observed throughout a cross-section of the gel, while a gradient in fluorescence is observed after 5 min of irradiation (Fig. 2d). Using the measured values for τ (Fig. 2a inset) and accounting for spatially varying light intensities via the Beer-Lambert law, the corresponding profiles in the crosslinking density gradient were predicted as a function of exposure time. In general, a large array of biologically relevant property gradients can be generated in this manner, by manipulating irradiation parameters such as wavelength, intensity, and time. For example, varying the steepness and absolute magnitude of crosslinking density gradients in the x - y plane may be useful for studying cell migration on surfaces, while patterning gradients in the z -direction allows the user to investigate the effect of crosslinking density on cell morphology in 3D.

Beyond controlling the gel's crosslinking density and subsequent material properties, the ability to direct gel erosion (i.e., complete mass loss) to create voids and channels within a cell-laden material environment would be highly useful. Such three-dimensional cell culture systems would afford the opportunity to spatially and temporally direct process extension, migration, or even cell-cell interactions. However, erosion is dependent on

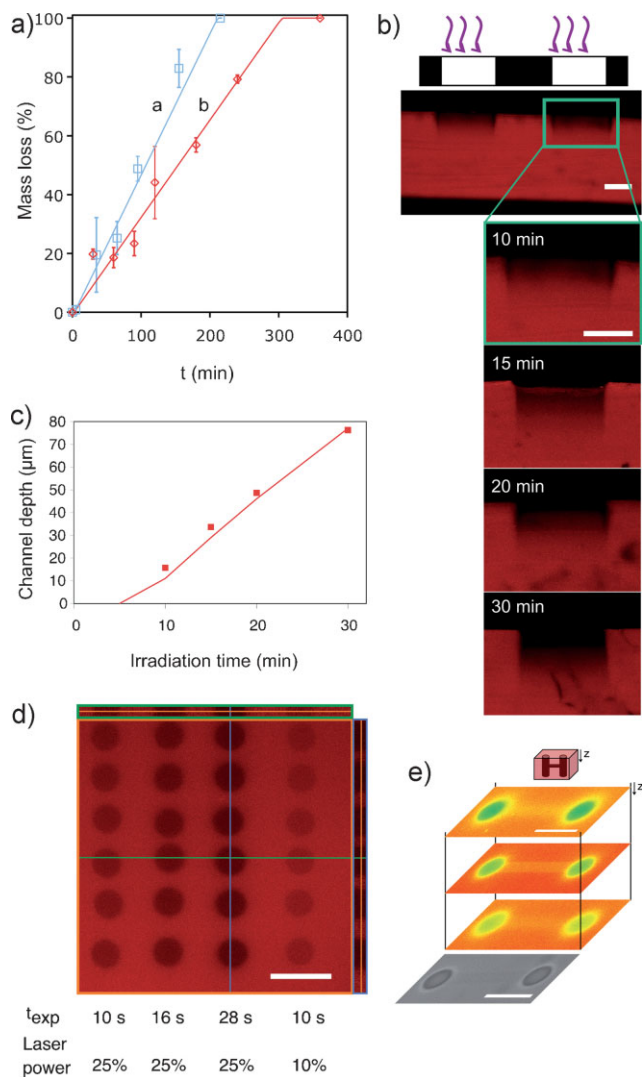


Figure 3. Hydrogel spatial erosion. a) Mass loss profile and time to complete degradation with irradiation (365 nm at 20 mW cm⁻²) were adjusted with the initial crosslinker concentration and agree well with predictions based on τ (solid lines): 15 wt% total macromer with (a) 10 and (b) 25 mol% photodegradable crosslinker. b) Photolithography (365 nm at 10 mW cm⁻² through 400 μ m clear lines separated by 400 μ m black lines) was used for spatially specific erosion, creating channels of increasing depth with increasing irradiation, (confocal images of the gel cross-section with irradiation time noted). c) The observed eroded channel depth (squares) compares well with channel depths predicted with τ and the photodegradation model (solid line). d) Spatial erosion of cylinders within a hydrogel was achieved using 405 nm laser on a LSM (top-down view of confocal stack with corresponding cross-sections marked by blue and green lines). Each column of cylinders is a different irradiation condition with decreasing scan speed and increasing laser power resulting in increased mass loss (left to right, scan time per plane and laser power (a) 10 s and 25%, (b) 16 s and 25%, (c) 28 s and 25%, and (d) 10 s and 10%). e) Similarly, vertical cylinders were degraded within a hydrogel (scan time 2 s per plane, 25% laser power, 100 μ m z-scan) and subsequently connected with a horizontal channel within the hydrogel (scan time 16 s per plane, 1 μ m z-scan) (confocal slices false colored to aid in visualization, with red indicating most fluorescence intensity (no degradation) and yellow to green least fluorescence (most degradation and mass loss). The presence of the structure within the hydrogel was verified in brightfield. All scale bars are 100 μ m.

concentration, where increased crosslinker concentration increases the time to complete degradation. These profiles compare well to model predictions based on τ and the gel connectivity (Fig. 3a). Further, spatially specific surface erosion was achieved with photolithography. Channels were degraded into a hydrogel by irradiation with a highly absorbed wavelength through a periodic photomask (400 μ m lines). Erosion of the hydrogel increases with irradiation time, as channels of increasing depth are generated (Fig. 3b). The channel depth was quantified with profilometry and increased linearly with irradiation time, which compares well to predicted erosion based on τ (Fig. 3c).

Upon characterizing τ and t_{rev} for this photodegradable hydrogel system, one can select other irradiating wavelengths of interest, especially those that would allow three-dimensional patterning in real time using common lasers and scanning speeds. While erosion takes several minutes using low intensity 365 nm light, higher intensity focused lasers allow more rapid gel erosion. In particular, region of interest functionality on a LSM (405 nm, 30 mW laser) was used to scan shapes within individual planes in the gel, locally eroding the polymer network. These shapes were subsequently scanned in the z-direction to create a three-dimensional void. The rate of degradation was dictated by the irradiation dose, which was controlled with the laser scan speed and power. Increased degradation and x-y plane resolution were observed with decreased scan speed (i.e., increased irradiation time) or increased laser power (i.e., increased irradiation intensity, I_0) (Fig. 3d), where cylinders were degraded in the hydrogel with 5 μ m z-scans. Scan times for erosion with the 405 nm laser are consistent with calculated values of τ , where 25–10% of the laser power corresponds to a τ of 0.2–0.4 ms per plane and a t_{rev} of 50–130 s per plane. Experimentally, complete degradation is observed with 10–30 s of exposure per plane. This faster erosion is likely due to underestimates of the laser focal point intensity and/or overlapping regions of out-of-focus light during z-scans. With these t_{rev} predictions, varying scan speeds and z-scan lengths were subsequently utilized to create connected channels within a hydrogel, where vertical cylinders connected by a horizontal channel were degraded within the hydrogel (Fig. 3e). This three-dimensional erosion with focused light can be predicted and utilized to create structures within a hydrogel, such as a channel connecting two cells. Total patterning of the hydrogel is complete in a few minutes.

To examine how precise, predictable changes in the gel microenvironment (i.e., crosslinking density) influence cell morphology, human mesenchymal stem cells (hMSCs) were encapsulated in photodegradable or non-degradable hydrogels. A portion of the photodegradable gels was subsequently flood irradiated on day 1 to create a z-direction crosslinking density gradient via degradation. The remaining photodegradable hydrogels were cultured without irradiation as a control for non-specific cell-induced degradation, while the non-degradable gels were irradiated as a control for non-specific light-induced degradation. Photodegradation and the corresponding change in crosslinking density lead to an increase in the molecular porosity of the hydrogel, or mesh size, and a decrease in the polymer density surrounding the cells, which have been previously shown to influence numerous cell functions such as cell morphology and spreading,^[9] viability,^[25] and diffusion of secreted molecules.^[26]

Upon irradiation and degradation on Day 1, no significant change in cell viability was observed (Supporting Information, Fig. S1), demonstrating the cytocompatibility of the photodegradation reaction and degradation products in vitro. In addition, cell spreading was observed over 4 days (Fig. S3) within the upper region of the degraded gel (top 100 μm , Fig. 4a), where the crosslinking density is lowered due to the z-direction degradation gradient (Fig. 2d). No spreading is observed in control gels that were not irradiated over 4 days, which is expected since the polymer density in the non-degraded gels should be too high to allow cell spreading (Fig. 4b, Fig. S2). This change in spreading was quantified, where an average cell area of 706 ± 77 and $473 \pm 94 \mu\text{m}^2$ were observed with and without irradiation, respectively. Furthermore, cell spreading and area were observed to be greatest in the upper regions of the gel, correlating with the z-direction degradation gradient, while no correlation of cell area with z-position was observed in non-degraded gels (Fig 4d). These

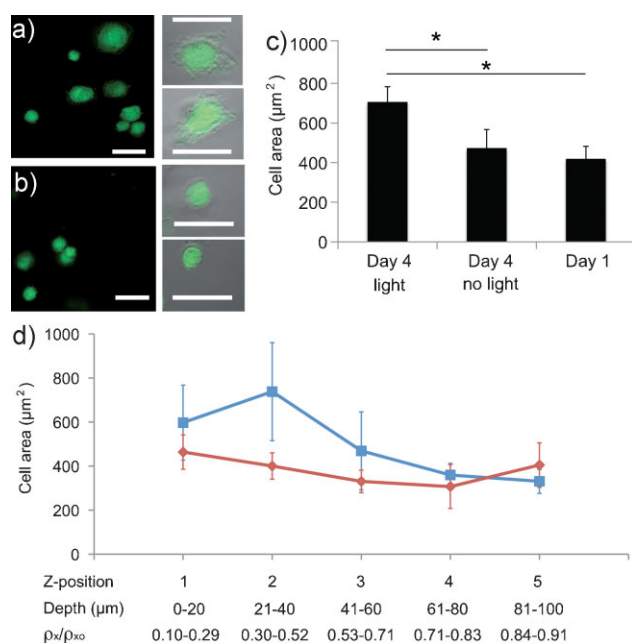


Figure 4. Cell area and morphology in gradient degraded hydrogels. hMSCs were encapsulated in photodegradable hydrogels and irradiated (365 nm at 10 mW cm^{-2} for 8 min) on day 1 to create a crosslinking density gradient in the z-direction. a) By Day 4, cell spreading is observed within the upper portion of the irradiated hydrogel (top $\sim 100 \mu\text{m}$), which possesses a significantly decreased crosslinking density based on predictions shown in Fig. 2, whereas limited spreading is observed in b) degradable gels without irradiation (top down view of confocal LSM stack). Changes in cell morphology were confirmed with brightfield images (right). Scale bars are $50 \mu\text{m}$. c) No change in cell area was observed over 4 days without irradiation (Day 1 prior to irradiation, day 4 no light). In contrast, an increase in cell area was observed with irradiation and degradation (Day 4 light) as compared to these controls ($* p < 0.1$). d) Spreading in response to the crosslinking density gradient ($\rho_x/\rho_{x0} = 0.1-0.9$, $\rho_{x0} = 0.006 \text{ M}$) was examined by splitting the $100 \mu\text{m}$ thick confocal stack into $20 \mu\text{m}$ thick confocal projections (top $20 \mu\text{m}$ of the gel = position 1). On Day 4, increased cell area was observed in the top of the gel as compared to the lower regions in irradiated samples (blue squares), whereas no change in cell area was observed in the z-direction without irradiation (red diamonds, $\rho_x/\rho_{x0} = 1$ at all positions).

photodegradable gels can be used to further explore the influence of hydrogel structure and polymer density on cell morphology, on other cell functions such as cytoskeletal organization and differentiation, or on ECM elaboration via gradient degradation.

Photodegradable hydrogels were synthesized, and their degradation kinetics in response to low-intensity irradiation was characterized via rheometry to determine rate constants for predicting changes in crosslinking density and mass loss. These hydrogels were degraded under cytocompatible irradiation conditions to create z- or x-direction property gradients, as well as to predictably erode hydrogels for controlled mass loss at any point in time and in three dimensions. Cell spreading was directed with a z-direction degradation gradient, where encapsulated cell area was greatest in the most highly degraded regions of the gel. These photodegradable gels can be used for culturing cells in three dimensions and allowing real-time, externally triggered manipulation of the cell microenvironment to examine its dynamic effect on cell function.

Experimental

Experimental methods can be found in the Supporting Information. This Experimental section includes (i) hydrogel synthesis, (ii) gel degradation characterization and modeling, (iii) gradient, photolithographic, and three-dimensional degradation, and (iv) cell encapsulation and three-dimensional culture.

Acknowledgements

The authors would like to thank Prof. C. N. Bowman for use of the rheometer and AFM. The authors acknowledge the NIH (DE012998 DE016523) and HHMI for funding this work. A. M. Kloxin acknowledges NASA GSRP and DoEd GAANN fellowships for funding. M. W. Tibbitt acknowledges DoEd GAANN fellowship for funding. Supporting Information is available online from Wiley InterScience or from the author.

Received: March 16, 2009

Revised: May 12, 2009

Published online:

- [1] J. L. Drury, D. J. Mooney, *Biomaterials* **2003**, *24*, 4337.
- [2] C. R. Nuttelman, M. A. Rice, A. E. Rydholm, C. N. Salinas, D. N. Shah, K. S. Anseth, *Prog. Polym. Sci.* **2008**, *33*, 167.
- [3] D. A. Wang, S. Varghese, B. Sharma, I. Strehin, S. Fermanian, J. Gorham, D. H. Fairbrother, B. Cascio, J. H. Elisseeff, *Nat. Mater.* **2007**, *6*, 385.
- [4] N. A. Peppas, J. Z. Hilt, A. Khademhosseini, R. Langer, *Adv. Mater.* **2006**, *18*, 1345.
- [5] D. S. W. Benoit, C. R. Nuttelman, S. D. Collins, K. S. Anseth, *Biomaterials* **2006**, *27*, 6102.
- [6] M. S. Hahn, J. S. Miller, J. L. West, *Adv. Mater.* **2005**, *17*, 2939.
- [7] P. Tayalia, C. R. Mendonca, T. Baldacchini, D. J. Mooney, E. Mazur, *Adv. Mater.* **2008**, *20*, 4494.
- [8] G. P. Raeber, M. P. Lutolf, J. A. Hubbell, *Acta Biomater.* **2007**, *3*, 615.
- [9] M. J. Mahoney, K. S. Anseth, *Biomaterials* **2006**, *27*, 2265.
- [10] C. Adeloew, T. Segura, J. A. Hubbell, P. Frey, *Biomaterials* **2008**, *29*, 314.
- [11] A. T. Metters, K. S. Anseth, C. N. Bowman, *Polymer* **2000**, *41*, 3993.
- [12] C. R. Nuttelman, A. M. Kloxin, K. S. Anseth, in *Tissue Eng.*, Vol. **585**, **2006**, 135.

- [13] K. A. Davis, K. S. Anseth, *Crit. Rev. Ther. Drug Carrier Syst.* **2002**, *19*, 385.
- [14] D. Seliktar, A. H. Zisch, M. P. Lutolf, J. L. Wrana, J. A. Hubbell, *J. Biomed. Mater. Res, Part A* **2004**, *68A*, 704.
- [15] F. M. Andreopoulos, C. R. Deible, M. T. Stauffer, S. G. Weber, W. R. Wagner, E. J. Beckman, A. J. Russell, *J. Am. Chem. Soc.* **1996**, *118*, 6235.
- [16] Y. J. Zheng, M. Miele, S. V. Mello, M. Mabrouki, F. M. Andreopoulos, V. Konka, S. M. Pham, R. M. Leblanc, *Macromolecules* **2002**, *35*, 5228.
- [17] Y. Luo, M. S. Shoichet, *Nat. Mater.* **2004**, *3*, 249.
- [18] A. M. Kloxin, A. M. Kasko, C. N. Salinas, K. S. Anseth, *Science* **2009**, *324*, 59.
- [19] Y. R. Zhao, Q. Zheng, K. Dakin, K. Xu, M. L. Martinez, W. H. Li, *J. Am. Chem. Soc.* **2004**, *126*, 4653.
- [20] C. P. Holmes, *J. Org. Chem.* **1997**, *62*, 2370.
- [21] A. T. Metters, C. N. Bowman, K. S. Anseth, *J. Phys. Chem. B* **2000**, *104*, 7043.
- [22] G. Odian, *Principles of polymerization*, John Wiley & Sons, Inc, Hoboken, New Jersey **2004**.
- [23] R. J. Young, P. A. Lovell, *Introduction to polymers*, Chapman & Hall, London, U.K **1991**.
- [24] S. J. Bryant, C. R. Nuttelman, K. S. Anseth, *J. Biomater. Sci, Polym. Ed.* **2000**, *11*, 439.
- [25] G. A. Hudalla, T. S. Eng, W. L. Murphy, *Biomacromolecules* **2008**, *9*, 842.
- [26] S. J. Bryant, R. J. Bender, K. L. Durand, K. S. Anseth, *Biotechnol. Bioeng.* **2004**, *86*, 747.
-